Process modeling of composites by resin transfer molding

Sensitivity analysis for non-isothermal considerations

B.J. Henz
US Army Research Laboratory, Aberdeen Proving Grounds, Aberdeen, Maryland, USA

K.K. Tamma
Department of Mechanical Engineering, University of Minnesota, Minneapolis, Minnesota, USA

R.V. Mohan
Department of Mechanical Engineering, North Carolina A&T University, Grensbro, North Carolina, USA, and

N.D. Ngo
United Defense, L.P., Minneapolis, Minnesota, USA

Received January 2003
Reviewed November 2003
Accepted December 2004

Abstract

Purpose – The purpose of the present paper is to describe the modeling, analysis and simulations for the resin transfer molding (RTM), manufacturing process with particular emphasis on the sensitivity analysis for non-isothermal applications.

Design/methodology/approach – For the manufacturing of advanced composites via RTM, besides the tracking of the resin flow fronts through a porous fiber perform, the heat transfer and the resin cure kinetics play an important role. The computational modeling is coupled multi-disciplinary problem of flow-thermal-cure. The paper describes the so-called continuous sensitivity formulation via the finite element method for this multi-disciplinary problem for process modeling of composites manufactured by RTM to predict, analyze and optimize the manufacturing process.

The authors are very pleased to acknowledge the support in part by Battelle/US Army Research Office (ARO), Research Triangle Park, North Carolina, under grant number DAAH04-96-C-0086, and by the Army High Performance Computing Research Center (AHPCRC) under the auspices of the Department of the Army, Army Research Laboratory (ARL) cooperative agreement number DAAH04-95-2-0003/contract number DAAH04-95-C-0008. The content does not necessarily reflect the position or the policy of the government, and no official endorsement should be inferred. Support in part by Dr Andrew Mark of the integrated modeling and testing (IMT) computational technical activity and the ARL/MSRC facilities are also gratefully acknowledged. Special thanks are due to the Computational and Information Sciences Directorate (CISD) and the Materials Division at the US Army Research Laboratory (ARL), Aberdeen Proving Ground, Maryland. Other related support in form of computer grants from the Minnesota Supercomputer Institute (MSI), Minneapolis, Minnesota is also gratefully acknowledged.

International Journal of Numerical Methods for Heat & Fluid Flow
Vol. 15 No. 7, 2005
pp. 631-653

0961-5539
DOI 10.1108/09615530510613852

Findings – Illustrative numerical examples are presented for two sample problems which include examination of sensitivity parameters for the case of material and geometric properties, and boundary conditions including fill time sensitivity analysis. The results indicate that the proposed formulations serve a useful role for the design and optimization of the RTM manufacturing process, thereby, avoiding heuristic trial-and-error methods.

Research limitations/implications – The paper restricts attention to constant properties and extensions to non-linear thermophysical properties will serve as an added benefit.

Practical implications – The present efforts significantly impact the design/optimization process in the process modeling of composites manufactured by RTM.

Originality/value – To the authors' knowledge, this is the first time that continuous sensitivity analysis is done for non-isothermal considerations in RTM.

Keywords Composite materials, Finite element analysis, Resins

Paper type Research paper

1. Introduction

Process modeling employing resin transfer molding (RTM) to manufacture complex structural geometries involves the injection of a polymer resin into a porous fibrous perform conforming to the geometry of the manufactured part. The mold is normally at a higher temperature than the resin and therefore the analysis of this process requires accounting for both the flow and thermal-kinetic equations. The solutions of these equations provide the flow front position, resin pressure, temperature and cure information to the analyst. After the results from the numerical analysis are collected, a systematic process of optimization can be performed with the assistance of the continuous sensitivity equation (CSE), thereby, avoiding heuristic trial-and-error methods.

Previously, the isothermal RTM CSE has been investigated by the authors Henz *et al.* (2003), and others (Mathur *et al.*, 2000). In this paper, the focus is on the non-isothermal RTM process and the derivation of the associated CSE. Detailed analysis of the non-isothermal process can be found in Lee *et al.* (1994), Kamal and Sourour (1973a, b), Ngo *et al.* (1998), Ngo and Tamma (n.d.), Lim and Lee (2000) and Shojaei *et al.* (2003). Derivation and analysis of the CSE for non-isothermal considerations has not been investigated previously and is now presented here for the first time.

Initially, an overview of the heat transfer and resin cure kinetics is given and solved numerically. After this brief overview, the CSE for the resin flow model coupled with the heat transfer and cure kinetics models is presented. After the numerical derivation some illustrative numerical results are presented for two sample axi-symmetric geometries including verification of the fill time sensitivity for a sensitivity parameter of inlet temperature.

2. Non-isothermal resin transfer molding

In this section, the temperature and cure model equations are described for non-isothermal RTM filling. Non-isothermal effects are an important consideration in many manufacturing process modeling applications employing RTM. Heat is transferred via various mechanisms of transport during the mold filling process. These mechanisms include convection from the mold walls, advection from the fluid, radiation to and from the mold, and heat generated by the exothermic curing process of the resin. For non-isothermal considerations, the independent parameters include

permeability and inlet pressure or flow rate. The dependent variables are the conductivity, viscosity, temperature, and degree of resin cure.

The first step to developing the so-called CSE for the non-isothermal filling process is to start with the governing model differential equations. By assuming that the fiber and resin temperatures are at the same equilibrium temperature inside a small control volume (Lee *et al.*, 1994), the energy balance can be written as

$$\rho c_p \frac{\partial T}{\partial t} + \rho_r c_{pr}(\mathbf{u}\cdot\nabla T) = \nabla\cdot k_{eff}\nabla T + \Phi\dot{G} \tag{1}$$

where $\dot{G}$ is the heat generated from the curing of the resin and Φ is the porosity of the fibrous preform. The average material properties are computed by

$$\begin{aligned} \rho c_p &= \Phi\rho_r c_{pr} + (1-\Phi)\rho_f c_{pf} \\ k_{eff} &= k_s + k_D \\ k_s &= \Phi k_r + (1-\Phi)k_f \end{aligned} \tag{2}$$

where the subscripts f and r denote fiber and resin properties, respectively. The effective conductivity, k_{eff}, is defined by Kaviany (1991). k_D is the thermal dispersion conductivity due to mechanical dissipation. The effective conductivity is computed as

$$k_{eff} = \frac{k_f k_r}{k_f w_r + k_r w_f} \tag{3}$$

where

$$\begin{aligned} w_f &= 1 - w_r \\ w_r &= \frac{\frac{\Phi}{\rho_f}}{\frac{\Phi}{\rho_f} + \frac{(1-\Phi)}{\rho_r}} \end{aligned} \tag{4}$$

Equation (1) represents the equilibrium temperature model used for developing the finite element equations which can then be readily implemented and solved numerically. The boundary conditions for the non-isothermal mold-filling process are given as

$$\begin{aligned} T &= T_w \ \text{at mold wall} \\ T &= T_{r0} \ \text{during filling, at inlet} \\ k\frac{\partial T}{\partial \mathbf{n}} &= (1-\Phi)\rho_r c_{pr}\mathbf{u}\cdot\mathbf{n}(T_{f0} - T) \ \text{at resin front} \end{aligned} \tag{5}$$

where T_r is the temperature of the resin, T_w is the wall temperature, and $\mathbf{n}$ is the direction normal to the resin flow front. Another thermal computation required in modeling the non-isothermal RTM filling process is cure. The curing analysis begins with the species mass balance (Ngo *et al.*, 1998), and is given as

$$\Phi\frac{\partial \alpha}{\partial t} + \mathbf{u}\cdot\nabla\alpha = \Phi R_\alpha \tag{6}$$

Here, α is the degree of cure, $\mathbf{u}$ is the velocity field, and R_α is the rate of chemical reaction. The boundary conditions for the cure problem are given by

$$\alpha = 0 \text{ during filling, at the model inlet(s)} \tag{7}$$

Since curing is an exothermic process, the heat generated is calculated with the following equation (Kamal and Sourour, 1973a, c; Sourour and Kamal, 1972)

$$\dot{G} = H_{\mathrm{R}} R_{\alpha} \tag{8}$$

where the term R_{α} for the chosen resin system is given as follows (Dusi *et al.*, 1987)

$$R_{\alpha} = (K_1 + K_2 \alpha^{n1})(1 - \alpha)^{n2} \tag{9}$$

and H_{R} is the heat of reaction per unit volume for the pure resin. The constants K_1 and K_2 are assumed as

$$\begin{aligned} K_1 &= A_1 \exp\left(-\frac{E_1}{RT}\right) \\ K_2 &= A_2 \exp\left(-\frac{E_2}{RT}\right) \end{aligned} \tag{10}$$

where A_1, A_2, E_1, E_2, n_1, and n_2 are the kinetic constants determined experimentally for each resin system used. The resin viscosity is a function of the degree of cure and temperature. The model used for calculating the viscosity of the present resin system is given as (Castro and Macosko, 1980)

$$\mu = A_{\mu} \exp\left(\frac{E_{\mu}}{RT}\right)\left(\frac{\alpha_g}{\alpha_g - \alpha}\right)^{A+B_{\alpha}} \tag{11}$$

which is used in conjunction with the implicit filling technique due to Mohan *et al.* (1999). This method has proven to be an effective approach for the solution of this class of problems.

Continuing with the development of the heat transfer finite element equations, we begin with the thermal equilibrium model in equation (1) and employ the method of weighted residuals. Thus,

$$\int_{\Omega} \mathbf{W}^T \left[\rho c_p \frac{\partial T}{\partial t} + \rho_{\mathrm{r}} c_{\mathrm{pr}} (\mathbf{u} \cdot T) - \nabla \cdot k \nabla T - \Phi \dot{G}\right] \mathrm{d}\Omega = 0 \tag{12}$$

Separating the terms and integrating by parts yields

$$\begin{aligned} &\int_{\Omega} \mathbf{W}^T \rho c_p \frac{\partial T}{\partial t} \mathrm{d}\Omega + \int_{\Omega} \mathbf{W}^T \rho_{\mathrm{r}} c_{\mathrm{pr}} (\mathbf{u} \cdot \nabla T) \mathrm{d}\Omega - \int_{\Gamma} \mathbf{W}^T (k \nabla T \cdot \mathbf{n}) \mathrm{d}\Gamma \\ &\quad + \int_{\Omega} \nabla \mathbf{W}^T k \nabla T \, \mathrm{d}\Omega - \int_{\Omega} \mathbf{W}^T \Phi \dot{G} \, \mathrm{d}\Omega = 0 \end{aligned} \tag{13}$$

Defining the weighting functions $\mathbf{W}$ to be the streamline upwind Petrov-Galerkin (SUPG) (Brooks and Hughes, 1982) weighting functions $\mathbf{N} + \lambda(\mathbf{u} \cdot \nabla \mathbf{N})$, and interpolating for T yields

$$\mathbf{W} = \mathbf{N} + \lambda(\mathbf{u}\cdot\nabla\mathbf{N})$$
$$\mathbf{T} = \sum_{i=1}^{\text{num}\cdot\text{nodes}} \mathbf{W}_i T_i \tag{14}$$

where i represents the associated node numbers. The heat flux, $\mathbf{q}$, is defined as

$$k\nabla T\cdot\mathbf{n} = -\mathbf{q}\cdot\mathbf{n} \tag{15}$$

Substituting equations (14) and (15) into equation (13) yields

$$\left[\int_\Omega \mathbf{W}\rho c_p\mathbf{N}\,\mathrm{d}\Omega\right]\frac{\partial\mathbf{T}}{\partial t} + \left[\int_\Omega \mathbf{W}\rho_r c_{pr}(\mathbf{u}\cdot\nabla\mathbf{N})\mathrm{d}\Omega\right]\mathbf{T} + \left[\int_\Omega \nabla\mathbf{W}k\nabla\mathbf{N}\,\mathrm{d}\Omega\right]\mathbf{T} = \int_\Gamma \mathbf{W}(k\nabla T\cdot\mathbf{n})\mathrm{d}\Gamma + \int_\Omega \mathbf{W}\boldsymbol{\Phi}\dot{G}\,\mathrm{d}\Omega \tag{16}$$

For the temperature analysis, the resulting semi-discretized equation is thus obtained as

$$\mathbf{C}\dot{\mathbf{T}} + (\mathbf{K}_{\text{ad}} + \mathbf{K}_{\text{cond}})\mathbf{T} = \mathbf{Q}_q + \mathbf{Q}_{\dot{G}} \tag{17}$$

where the terms in equation (17) are defined as

$$\begin{aligned}
\mathbf{C} &= \int_\Omega \mathbf{W}^T\rho c_p\mathbf{N}\,\mathrm{d}\Omega\\
\mathbf{K}_{\text{ad}} &= \int_\Omega \mathbf{W}^T\rho c_{pr}(\mathbf{u}\cdot\mathbf{B}_N)\mathrm{d}\Omega\\
\mathbf{K}_{\text{cond}} &= \int_\Omega \mathbf{B}_{\mathbf{W}}^T k\mathbf{B}_N\mathrm{d}\Omega\\
\mathbf{Q}_q &= \int_\Gamma \mathbf{W}^T(-\mathbf{q}\cdot\mathbf{n})\mathrm{d}\Gamma\\
\mathbf{Q}_{\dot{G}} &= \int_\Omega \mathbf{W}^T\Phi\dot{G}\,\mathrm{d}\Omega
\end{aligned} \tag{18}$$

where k is the effective permeability, k_{eff}, from equation (2). The time discretization for the temperature analysis is employed, for an arbitrary θ, as

$$\dot{\mathbf{T}}_\theta = \frac{\mathbf{T}_{n+1} - \mathbf{T}_n}{\Delta t} \tag{19}$$

The cure model equation is also solved using the finite element method. Applying the method of weighted residuals on the species mass balance in equation (6) yields

$$\int_\Omega \mathbf{W}^T\left(\Phi\frac{\partial\alpha}{\partial t} + \mathbf{u}\cdot\nabla\alpha - \Phi R_\alpha\right)\mathrm{d}\Omega = 0 \tag{20}$$

subsequently separating terms and integrating by parts yields

$$\int_{\Omega} \mathbf{W}^T \Phi \frac{\partial \alpha}{\partial t} \mathrm{d}\Omega + \int_{\Omega} \mathbf{W}^T \mathbf{u} \cdot \nabla \alpha \, \mathrm{d}\Omega - \int_{\Omega} \Phi R_{\alpha} \, \mathrm{d}\Omega = 0 \tag{21}$$

As in the temperature problem, the weighting functions $\mathbf{W}$ are defined as the SUPG weighting functions $\mathbf{N} + \lambda(\mathbf{u} \cdot \nabla \mathbf{N})$, and interpolating for α yields

$$\begin{aligned} \mathbf{W} &= \mathbf{N} + \lambda(\mathbf{u} \cdot \nabla \mathbf{N}) \\ \alpha &= \sum_{i=1}^{\text{num} \cdot \text{nodes}} \mathbf{W}_i \alpha_i \end{aligned} \tag{22}$$

Rewriting equation (21) in the semi-discretized form results in

$$\mathbf{C}\dot{\alpha} + \mathbf{K}\alpha = \mathbf{Q}_{R_{\alpha}} \tag{23}$$

where the terms in equation (23) are defined as

$$\begin{aligned} \mathbf{C} &= \int_{\Omega} \Phi \mathbf{W}^T \mathbf{N} \, \mathrm{d}\Omega \\ \mathbf{K} &= \int_{\Omega} \mathbf{W}^T (\mathbf{u} \cdot \mathbf{B}_N) \mathrm{d}\Omega \\ \mathbf{Q}_{R_{\alpha}} &= \int_{\Omega} \Phi \mathbf{W}^T R_{\alpha} \, \mathrm{d}\Omega \end{aligned} \tag{24}$$

The time discretization for the cure analysis is employed, for an arbitrary θ, as

$$\dot{\alpha}_{\theta} = \frac{\alpha_{n+1} - \alpha_n}{\Delta t} \tag{25}$$

A more detailed discussion of the non-isothermal RTM computational analysis can be found in Ngo *et al.* (1998).

3. Sensitivity analysis of non-isothermal resin transfer molding

In this section the CSE for non-isothermal RTM filling, temperature, and cure are defined. The computational procedure for the non-isothermal RTM filling problem is described along with some illustrative results from an example axi-symmetric model. Finally, the fill time sensitivity with respect to the inlet temperature is discussed and verified with the use of an additional axi-symmetric example.

3.1 RTM filling sensitivity

The semi-discretized equation for mold filling is given by

$$\mathbf{KP} = \mathbf{q} \tag{26}$$

For the non-isothermal pressure sensitivity calculation, viscosity is a function of temperature and cure (i.e. $\mu(T, \alpha)$). The sensitivity equation for RTM filling is given by the following semi-discretized equation as

$$\frac{\partial \mathbf{K}}{\partial p}\mathbf{P} + \mathbf{K}\mathbf{S}_P = \mathbf{S}_q \tag{27}$$

where p is the specified sensitivity parameter. Equation (27) is the same CSE as is used in isothermal filling simulations and the derivation thereof is given in the aforementioned isothermal references (Henz *et al.*, 2003; Mathur *et al.*, 2000). The terms $\partial k/\partial p$, $\mathbf{K}$, and $\mathbf{S}_q$ from equation (27) are defined as

$$\frac{\partial \mathbf{K}}{\partial p} = \int_{\Omega} \mathbf{B}^T \frac{\partial \bar{\mathbf{K}}}{\partial p} \frac{1}{\mu} \mathbf{B}\, d\Omega + \int_{\Omega} \mathbf{B}^T \bar{\mathbf{K}} \left(-\frac{1}{\mu^2} \right) \frac{\partial \mu}{\partial p} \mathbf{B}\, d\Omega$$

$$\mathbf{K} = \int_{\Omega} \mathbf{B}^T \frac{\bar{\mathbf{K}}}{\mu} \mathbf{B}\, d\Omega$$

$$\mathbf{S}_q = \int_{\Gamma} \mathbf{N}^T \frac{\partial \bar{\mathbf{K}}}{\partial p} \frac{1}{\mu} \cdot \nabla P \cdot \mathbf{n} d\Gamma + \int_{\Gamma} \mathbf{N}^{\mathbf{T}} \bar{\mathbf{K}} \frac{\partial}{\partial p} \left(\frac{1}{\mu} \right) \cdot \nabla P \cdot \mathbf{n} d\Gamma + \int_{\Gamma} \mathbf{N}^T \frac{\bar{\mathbf{K}}}{\mu} \cdot \nabla \mathbf{S}_P \cdot \mathbf{n}\, d\Gamma \tag{28}$$

In equation (28) $\bar{\mathbf{K}}$ is the permeability tensor of the fiber perform. With the viscosity defined as a function of temperature and cure, this leads to an additional term in the non-isothermal RTM filling CSE, namely $\frac{\partial}{\partial p}\left(\frac{1}{\mu(T,\alpha)}\right)$

$$\frac{\partial \mathbf{K}}{\partial p} = \int_{\Omega} \mathbf{B}^{\mathbf{T}} \frac{\partial \bar{\mathbf{K}}}{\partial p} \frac{1}{\mu} \mathbf{B}\, d\Omega + \int_{\Omega} \mathbf{B}^{\mathbf{T}} \bar{\mathbf{K}} \left(-\frac{1}{\mu^2} \right) \frac{\partial \mu(T, \alpha)}{\partial p} \mathbf{B}\, d\Omega \tag{29}$$

where $(\partial \mu(T, \alpha))/\partial p$ is defined as

$$\frac{\partial \mu(T(p), \alpha(p); p)}{\partial p} = \frac{\partial \mu}{\partial p} + A_\mu \left(\frac{\alpha_g}{\alpha_g - \alpha} \right)^{A+B_\alpha} \left[-\frac{E_\mu}{RT^2} e^{\left(\frac{E_\mu}{RT}\right)} \right] \frac{\partial T}{\partial p} + A_\mu e^{\left(\frac{E_\mu}{RT}\right)} \left[\left(\frac{\alpha_g}{\alpha_g - \alpha} \right)^{A+B_\alpha} \left[-\frac{A + B_\alpha}{\alpha_g - \alpha} + B_\alpha \ln \left(\frac{\alpha_g}{\alpha_g - \alpha} \right) \right] \right] \frac{\partial \alpha}{\partial p} \tag{30}$$

Note, that for $\mu = \text{constant}$, $\partial \mu/\partial p = 0$ where $\mu \neq p$, it will yield the same results as the isothermal model equation. In the non-isothermal filling simulations the temperature profile is also computed thereby allowing for the solution of the temperature sensitivity equations.

3.2 RTM temperature sensitivity

The temperature sensitivity is evaluated by taking the partial derivative of equation (1) with respect to the sensitivity parameter p.

$$\frac{\partial}{\partial p} \left[\rho c_p \frac{\partial T}{\partial t} + \rho_r c_{pr} (\mathbf{u} \cdot \nabla T) \right] = \frac{\partial}{\partial p} [\nabla \cdot k_{\text{eff}} \nabla T + \Phi \dot{G}] \tag{31}$$

This results in

$$\frac{\partial}{\partial p}(\rho c_p)\frac{\partial T}{\partial t}+\rho c_p\frac{\partial \mathbf{S}_T}{\partial t}+\frac{\partial}{\partial p}(\rho c_p)(\mathbf{u}\cdot\nabla T)+\rho_r c_{pr}\frac{\partial}{\partial p}(\mathbf{u}\cdot\nabla T)$$
$$=\nabla\cdot\frac{\partial k_{\text{eff}}}{\partial p}\nabla T+\nabla\cdot k_{\text{eff}}\nabla\mathbf{S}_T+\frac{\partial\Phi}{\partial p}\dot{G}+\Phi\frac{\partial\dot{G}}{\partial p} \tag{32}$$

where the temperature sensitivity is defined as, $\mathbf{S}_T \equiv \partial T/\partial p$.

Moving all the terms in equation (32) to the left hand side and applying the method of weighted residuals yields

$$\int_\Omega \mathbf{W}^T\left[\frac{\partial}{\partial p}(\rho c_p)\frac{\partial T}{\partial t}+\rho c_p\frac{\partial \mathbf{S}_T}{\partial t}+\frac{\partial}{\partial p}(\rho c_p)(\mathbf{u}\cdot\nabla T)+\rho_r c_{pr}\frac{\partial}{\partial p}(\mathbf{u}\cdot\nabla T)\right]d\Omega$$
$$-\int_\Omega \mathbf{W}^T\left[\nabla\cdot\frac{\partial k_{\text{eff}}}{\partial p}\nabla T+\nabla\cdot k_{\text{eff}}\nabla\mathbf{S}_T+\frac{\partial\Phi}{\partial p}\dot{G}+\Phi\frac{\partial\dot{G}}{\partial p}\right]d\Omega=0 \tag{33}$$

Before deriving the finite element equations, the partial derivative of the boundary conditions for the temperature analysis need to be computed. For the temperature analysis, equation (32), the boundary conditions are given as

$$\mathbf{S}_T=\frac{\partial T_w}{\partial p}\ \text{ at the mold wall}$$
$$\mathbf{S}_T=\frac{\partial T_{r0}}{\partial p}\ \text{ during filling, at mold inlet} \tag{34}$$
$$k_{\text{eff}}\frac{\partial \mathbf{S}_T}{\partial n}=\frac{\partial}{\partial p}((1-\Phi)\rho_r c_{pr}(\mathbf{u}\cdot\mathbf{n})(T_{f0}-T))\ \text{ at resin flow front}$$

After applying the Green-Gauss theorem to convert the volume integral to a surface integral, the temperature sensitivity equation is given as

$$\int_\Omega \mathbf{W}^T\frac{\partial}{\partial p}(\rho c_p)\frac{\partial T}{\partial t}d\Omega+\int_\Omega \mathbf{W}^T\rho c_p\frac{\partial \mathbf{S}_T}{\partial t}d\Omega+\int_\Omega \mathbf{W}^T\frac{\partial}{\partial p}(\rho_r c_{pr})(\mathbf{u}\cdot\nabla T)d\Omega$$
$$+\int_\Omega \mathbf{W}^T\rho_r c_{pr}\left(\frac{\partial \mathbf{u}}{\partial p}\cdot T\right)d\Omega+\int_\Omega \mathbf{W}^T\rho_r c_{pr}(\mathbf{u}\cdot\nabla\mathbf{S}_T)d\Omega-\int_\Gamma \mathbf{W}^T\left(\frac{\partial k_{\text{eff}}}{\partial p}\nabla T\cdot\mathbf{n}\right)d\Gamma$$
$$+\int_\Omega \nabla\mathbf{W}^T\cdot\frac{\partial k_{\text{eff}}}{\partial p}\nabla T d\Omega-\int_\Gamma \nabla\mathbf{W}^T(k_{\text{eff}}\nabla\mathbf{S}_T\cdot\mathbf{n})d\Gamma+\int_\Omega \nabla\mathbf{W}^T\cdot k_{\text{eff}}\nabla\mathbf{S}_T d\Omega$$
$$-\int_\Omega \mathbf{W}^T\frac{\partial\Phi}{\partial p}\dot{G}d\Omega-\int_\Omega \mathbf{W}^T\Phi\frac{\partial\dot{G}}{\partial p}d\Omega=0 \tag{35}$$

where ρc_p is defined in equation (2), and ρ_r and c_{pr} are resin material properties. Defining the weighting functions $\mathbf{W}$ be the SUPG weighting functions $\mathbf{N}+\lambda(\mathbf{u}\cdot\nabla\mathbf{N})$, and interpolating for $\mathbf{T}$ and $\mathbf{S}_T$ yields

$$\begin{aligned}\mathbf{W} &= \mathbf{N} + \lambda(\mathbf{u}\cdot\nabla\mathbf{N})\\ \mathbf{T} &= \sum_{i=1}^{\text{num}\cdot\text{nodes}} \mathbf{W}_i T_i\\ \mathbf{S}_T &= \sum_{i=1}^{\text{num}\cdot\text{nodes}} \mathbf{W}_i \mathbf{S}_{T_i}\end{aligned} \tag{36}$$

Substituting equation (36) into equation (35), yields the semi-discretized finite element equations for the temperature CSE, given as

$$\frac{\partial \mathbf{C}}{\partial p}\dot{\mathbf{T}} + \mathbf{C}\dot{\mathbf{S}}_T + \left(\frac{\partial \mathbf{K}_{\text{ad}}}{\partial p} + \frac{\partial \mathbf{K}_{\text{cond}}}{\partial p}\right)\mathbf{T} + (\mathbf{K}_{\text{ad}} + \mathbf{K}_{\text{cond}})\mathbf{S}_T = \mathbf{S}_q + \mathbf{S}_{\dot{G}} \tag{37}$$

where each of the terms in equation (37) are defined as

$$\begin{aligned}\frac{\partial \mathbf{C}}{\partial p} &= \int_\Omega \mathbf{W}^T \frac{\partial}{\partial p}(\rho c_p)\mathbf{N}\,\mathrm{d}\Omega\\ \mathbf{C} &= \int_\Omega \mathbf{W}^T(\rho c_p)\mathbf{N}\,\mathrm{d}\Omega\\ \frac{\partial \mathbf{K}_{\text{ad}}}{\partial p} &= \int_\Omega \mathbf{W}^T \frac{\partial}{\partial p}(\rho c_p)(\mathbf{u}\cdot\mathbf{B})\mathrm{d}\Omega + \int_\Omega \mathbf{W}^T(\rho_{\text{r}} c_{\text{pr}})\left(\frac{\partial \mathbf{u}}{\partial p}\cdot\mathbf{B}\right)\mathrm{d}\Omega\\ \mathbf{K}_{\text{ad}} &= \int_\Omega \mathbf{W}^T(\rho_{\text{r}} c_{\text{pr}})(\mathbf{u}\cdot\mathbf{B})\mathrm{d}\Omega\\ \frac{\partial \mathbf{K}_{\text{cond}}}{\partial p} &= \int_\Omega \mathbf{B}_{\mathbf{W}}^T \frac{\partial k_{\text{eff}}}{\partial p}\mathbf{B}\,\mathrm{d}\Omega\\ \mathbf{K}_{\text{cond}} &= \int_\Omega \mathbf{B}_{\mathbf{W}}^T k_{\text{eff}}\mathbf{B}\,\mathrm{d}\Omega\\ \mathbf{S}_q &= \int_\Gamma \mathbf{W}^T\left(\frac{\partial k_{\text{eff}}}{\partial p}\nabla T\cdot\mathbf{n}\right)\mathrm{d}\Gamma + \int_\Gamma \mathbf{W}^T(k_{\text{eff}}\nabla\mathbf{S}_T\cdot\mathbf{n})\mathrm{d}\Gamma\\ \mathbf{S}_{\dot{G}_\theta} &= \int_\Omega \mathbf{W}^T\frac{\partial \Phi}{\partial p}\dot{G}\,\mathrm{d}\Omega + \int_\Omega \mathbf{W}^T\Phi\frac{\partial \dot{G}}{\partial p}\mathrm{d}\Omega\end{aligned} \tag{38}$$

with heat generation, $\dot{G}$, defined in equation (8). The time discretization is employed as

$$\begin{aligned}\dot{\mathbf{T}}_\theta &= \frac{\mathbf{T}_{n+1} - \mathbf{T}_n}{\Delta t}\\ \dot{\mathbf{S}}_{T_\theta} &= \frac{\mathbf{S}_{T_{n+1}} - \mathbf{S}_{T_n}}{\Delta t}\end{aligned} \tag{39}$$

The fully discretized representations are thus given as

$$\begin{aligned}[\mathbf{C} + \theta\mathbf{K}\Delta t]\mathbf{S}_{T_{n+1}} = &-\left[\frac{\partial \mathbf{C}}{\partial p} + \theta\frac{\partial \mathbf{K}}{\partial p}\Delta t\right]\mathbf{T}_{n+1} + \left[\frac{\partial \mathbf{C}}{\partial p} - (1-\theta)\frac{\partial \mathbf{K}}{\partial p}\Delta t\right]\mathbf{T}_n\\ &+ [\mathbf{C} - (1-\theta)\mathbf{K}\Delta t]\mathbf{S}_{T_n} + \Delta t\left[(1-\theta)\frac{\partial \mathbf{F}_n}{\partial p} + \theta\frac{\partial \mathbf{F}_{n+1}}{\partial p}\right]\end{aligned} \tag{40}$$

with temperature T and temperature sensitivity $\mathbf{S}_T$ approximated by

$$\begin{aligned} \mathbf{T}_\theta &= (1-\theta)\mathbf{T}_n + \theta\mathbf{T}_{n+1} \\ \mathbf{S}_{T_\theta} &= (1-\theta)\mathbf{S}_{T_n} + \theta\mathbf{S}_{T_{n+1}} \end{aligned} \tag{41}$$

and $\mathbf{F}$ is defined as

$$\mathbf{F} = \mathbf{S}_q + \mathbf{S}_{\dot{G}} \tag{42}$$

Some of the terms required for calculating the temperature sensitivity must still be defined. The first of these comes from equation (3), where $\partial k_{\text{eff}}/\partial p$ is defined from the following equation for sensitivity parameter $p = k_{\text{r}}$,

$$\frac{\partial k_{\text{eff}}}{\partial p} = \frac{k_{\text{f}}}{k_{\text{f}}w_{\text{r}} + k_{\text{r}}w_{\text{f}}} - \frac{k_{\text{f}}k_{\text{r}}}{(k_{\text{f}}w_{\text{r}} + k_{\text{r}}w_{\text{f}})^2}\, w_{\text{f}} \tag{43}$$

or for $p = k_{\text{f}}$

$$\frac{\partial k_{\text{eff}}}{\partial p} = \frac{k_{\text{r}}}{k_{\text{f}}w_{\text{r}} + k_{\text{r}}w_{\text{f}}} - \frac{k_{\text{f}}k_{\text{r}}}{(k_{\text{f}}w_{\text{r}} + k_{\text{r}}w_{\text{f}})^2}\, w_{\text{r}} \tag{44}$$

The heat generation term, $\partial\dot{G}/\partial p$ is defined as

$$\frac{\partial \dot{G}}{\partial p} = H_{\text{R}}\frac{\partial R_\alpha}{\partial p} \tag{45}$$

where H_{R} is the heat of reaction per unit volume for the pure resin. The rate of reaction term, $\partial R_\alpha/\partial p$, is defined by

$$\begin{aligned} \frac{\partial}{\partial p}R_\alpha = &\left(\frac{\partial K_1}{\partial p} + \frac{\partial K_2}{\partial p}\,\alpha^{n_1} + K_2 n_1 \alpha^{n_1-1}\frac{\partial \alpha}{\partial p}\right)(1-\alpha)^{n_2} \\ &+ (K_1 + K_2\alpha^{n_1})n_2(1-\alpha)^{(n_2-1)}\frac{\partial \alpha}{\partial p} \end{aligned} \tag{46}$$

where $\partial k_1/\partial p$ and $\partial k_2/\partial p$ are computed by taking the partial derivative of K_1 and K_2 in equation (10) with respect to the sensitivity parameter p, i.e.

$$\begin{aligned} \frac{\partial K_1}{\partial p} &= \frac{E_1 A_1}{RT^2}\,\mathrm{e}^{\left(-\frac{E_1}{RT}\right)}\frac{\partial T}{\partial p} \\ \frac{\partial K_2}{\partial p} &= \frac{E_2 A_2}{RT^2}\,\mathrm{e}^{\left(-\frac{E_2}{RT}\right)}\frac{\partial T}{\partial p} \end{aligned} \tag{47}$$

Equation (40) is used to solve for the temperature sensitivity profile for each time step after the temperature results have been calculated.

3.3 RTM cure sensitivity

In the non-isothermal RTM analysis, cure is also computed. This leads to the following evaluation of the cure sensitivity equation. The cure sensitivity equation is computed by taking the partial derivative of equation (6) with respect to the sensitivity parameter p, i.e.

$$\frac{\partial}{\partial p}\left(\Phi\frac{\partial\alpha}{\partial t}+\mathbf{u}\cdot\nabla\alpha=\Phi R_\alpha\right) \tag{48}$$

which leads to

$$\frac{\partial\Phi}{\partial p}\frac{\partial\alpha}{\partial t}+\Phi\frac{\mathbf{S}_\alpha}{\partial t}+\frac{\partial\mathbf{u}}{\partial p}\cdot\nabla\alpha+\mathbf{u}\cdot\nabla\mathbf{S}_\alpha=\frac{\partial\Phi}{\partial p}R_\alpha+\Phi\frac{\partial R_\alpha}{\partial p} \tag{49}$$

where the cure sensitivity is defined as $\mathbf{S}_\alpha\equiv\partial\alpha/\partial p$. Applying the method of weighted residuals, we have

$$\int_\Omega\mathbf{W}^T\left(\frac{\partial\Phi}{\partial p}\frac{\partial\alpha}{\partial t}+\Phi\frac{\mathbf{S}_\alpha}{\partial t}+\frac{\partial\mathbf{u}}{\partial p}\cdot\nabla\alpha+\mathbf{u}\cdot\nabla\mathbf{S}_\alpha-\frac{\partial\Phi}{\partial p}R_\alpha-\Phi\frac{\partial R_\alpha}{\partial p}\right)\mathrm{d}\Omega=0 \tag{50}$$

As in the temperature problem, the weighting functions $\mathbf{W}$ are defined to be the SUPG weighting functions $\mathbf{N}+\lambda(\mathbf{u}\cdot\nabla\mathbf{N})$, and interpolating for α and $\mathbf{S}_\alpha$ yields

$$\begin{aligned}\mathbf{W}&=\mathbf{N}+\lambda(\mathbf{u}\cdot\nabla\mathbf{N})\\ \alpha&=\sum_{i=1}^{\text{num}\cdot\text{nodes}}\mathbf{W}_i\alpha_i\\ \mathbf{S}_\alpha&=\sum_{i=1}^{\text{num}\cdot\text{nodes}}\mathbf{W}_i\mathbf{S}_{\alpha_i}\end{aligned} \tag{51}$$

The semi-discretized cure sensitivity equation is thus given as

$$\frac{\partial\mathbf{C}}{\partial p}\dot{\alpha}+\mathbf{C}\dot{\mathbf{S}}_\alpha+\frac{\partial\mathbf{K}}{\partial p}\alpha+\mathbf{K}\mathbf{S}_\alpha=\frac{\partial\mathbf{Q}_{R_\alpha}}{\partial p} \tag{52}$$

where the terms in equation (52) are defined as

$$\begin{aligned}\mathbf{C}&=\int_\Omega\mathbf{\Phi}\mathbf{W}^T\mathbf{N}\,\mathrm{d}\Omega\\ \frac{\partial\mathbf{C}}{\partial p}&=\int_\Omega\frac{\partial\Phi}{\partial p}\mathbf{W}^T\mathbf{N}\,\mathrm{d}\Omega\\ \mathbf{K}&=\int_\Omega\mathbf{W}^T(\mathbf{u}\cdot\mathbf{B}_N)\mathrm{d}\Omega\\ \frac{\partial\mathbf{K}}{\partial p}&=\int_\Omega\mathbf{W}^T\left(\frac{\partial\mathbf{u}}{\partial p}\cdot\mathbf{B}_N\right)\mathrm{d}\Omega\\ \frac{\partial\mathbf{Q}_{R_\alpha}}{\partial p}&=\int_\Omega\frac{\partial\Phi}{\partial p}\mathbf{W}^TR_\alpha\mathrm{d}\Omega+\int_\Omega\Phi\mathbf{W}^T\frac{\partial R_\alpha}{\partial p}\mathrm{d}\Omega\end{aligned} \tag{53}$$

with the time discretization employed as

$$\begin{aligned}\dot{\alpha}_\theta&=\frac{\alpha_{n+1}-\alpha_n}{\Delta t}\\ \dot{\mathbf{S}}_{\alpha_\theta}&=\frac{\mathbf{S}_{\alpha_{n+1}}-\mathbf{S}_{\alpha_n}}{\Delta t}\end{aligned} \tag{54}$$

The boundary conditions for the cure CSE, equation (49), are computed as

$$\frac{\partial \alpha}{\partial p} = 0 \text{ during filling, at the model inlet(s)} \tag{55}$$

The cure sensitivity is solved numerically employing

$$\begin{aligned}[\mathbf{C} + \theta \mathbf{K} \Delta t]\mathbf{S}_{\alpha_{n+1}} = &- \left[\frac{\partial \mathbf{C}}{\partial p} + \theta \frac{\partial \mathbf{K}}{\partial p}\Delta t\right]\alpha_{n+1} + \left[\frac{\partial \mathbf{C}}{\partial p} - (1-\theta)\frac{\partial \mathbf{K}}{\partial p}\Delta t\right]\alpha_n \\ &+ [\mathbf{C} - (1-\theta)\mathbf{K}\Delta t]\mathbf{S}_{\alpha_n} + \Delta t\left[(1-\theta)\frac{\partial \mathbf{F}_n}{\partial p} + \theta \frac{\partial \mathbf{F}_{n+1}}{\partial p}\right]\end{aligned} \tag{56}$$

with cure α and cure sensitivity $\mathbf{S}_\alpha$ approximated by

$$\begin{aligned}\alpha_\theta &= (1-\theta)\alpha_n + \theta\alpha_{n+1} \\ \mathbf{S}_{\alpha_\theta} &= (1-\theta)\mathbf{S}_{\alpha_n} + \theta\mathbf{S}_{\alpha_{n+1}}\end{aligned} \tag{57}$$

All of the terms in equation (56) are defined in equations (24) and (53).

3.4 Computational procedure

The steps required to perform the sensitivity analysis for non-isothermal RTM process modeling are outlined below.

(1) The filling analysis is described by the semi-discretized equation, equation (26).

(2) For non-isothermal filling analysis include the necessary temperature and cure equations, equations (17) and (23), respectively.

(3) The CSE for the RTM filling simulation is given in semi-discretized form in equation (27).

(4) For the non-isothermal sensitivity analysis it is also necessary to take the partial derivative of the temperature and cure equations with respect to the sensitivity parameter p, equations (32) and (48). This results in the semi-discretized equations for temperature and cure sensitivity, equations (37) and (52), respectively.

(5) In order to solve the filling equation, the boundary conditions are defined as

$$\begin{aligned}&\frac{\partial P}{\partial \mathbf{n}} = 0 \text{ on mold walls} \\ &P = 0 \text{ at flow front} \\ &P = P_0 \text{ prescribed pressure at inlet} \\ &\text{or} \\ &q = q_0 \text{ prescribed flow rate at inlet}\end{aligned} \tag{58}$$

(6) To solve the filling sensitivity equations the boundary conditions must be computed by taking the partial derivatives of all filling boundary conditions given as

$$\frac{\partial}{\partial p}\left(\frac{\partial P}{\partial \mathbf{n}}\right) = 0 \text{ on mold walls}$$
$$\frac{\partial P}{\partial p} = 0 \text{ at flow front} \tag{59}$$
$$\frac{\partial P}{\partial p} = \frac{\partial P_0}{\partial p} \text{ for constant pressure at inlet}$$

or for constant flow at the inlet

$$\frac{\partial q}{\partial p} = \frac{\partial q_0}{\partial p} \text{ for constant flow rate at inlet}$$

(7) For the non-isothermal analysis the temperature and cure boundary conditions are required, and are defined in equations (5) and (7), respectively.

(8) For temperature and cure sensitivities the thermal boundary conditions need to be computed. The temperature sensitivity boundary conditions can be found in equation (34), with the cure sensitivity boundary conditions defined at the inlet as specified in equation (55).

(9) For the non-isothermal RTM sensitivity analysis, $\partial\mathbf{K}/\partial p$ and $\mathbf{S}_q$ must be computed and boundary conditions applied. The matrix $\partial\mathbf{K}/\partial p$ requires $\partial\bar{\mathbf{K}}/\partial p$ and $\partial\mu(T,\alpha)/\partial p$ as defined in equation (30). The values in vector $\mathbf{S}_q$ are set to zero except where the inlet flow rate has been defined.

(10) The temperature sensitivity analysis requires computation of five matrices and vectors including, $\partial\mathbf{C}/\partial p$, $\partial\mathbf{K}_{\text{ad}}/\partial p$, $\partial\mathbf{K}_{\text{cond}}/\partial p$, $\mathbf{S}_q$ and $\mathbf{S}_{\dot{G}}$. The values required for all of these terms can be found in equation (38).

(11) Similarly, for the cure sensitivity $\partial\mathbf{C}/\partial p$, $\partial\mathbf{K}/\partial p$, and $\partial\mathbf{Q}_{R_\alpha}/\partial p$ are required and are defined in equation (53).

(12) Once all of these equations are defined and the boundary conditions applied, the results must be obtained. First the pressure results are computed, followed by the pressure sensitivity results. After the filling is completed for the current time step the thermal computations are performed. The temperature and cure considerations are obtained first, followed by the temperature and cure sensitivities. Note that the temperature and cure time step is normally less than the filling time step (Ngo *et al.*, 1998).

(13) Before continuing on to the next filling step compute the new viscosity and viscosity sensitivity values from the thermal results and reform $\mathbf{K}$ and $\partial\mathbf{K}/\partial p$.

(14) Proceed to the next filling time step until the mold is completely filled. The filling time step in the flow model is arbitrary since the implicit pure finite element method employs the principle of time-dependent mass conservation of the resin. This differs from the control volume-finite element approach, in that any number of regions may be filled with resin during a given time step, instead of just one (unless symmetry conditions exist in which case a group of elements may be filled) as required by the quasi-steady state problem.

3.5 Example geometry with numerical results

An axi-symmetric example geometry is shown in Figure 1. The disk is injected with resin from inlets placed along the inside radius of the disk. By varying the inlet boundary conditions and the material properties it is possible to show how these variables affect the fill time or inlet pressure of the model. Observation of the results of the sensitivity values for these variables are used to indicate the qualitative and quantitative changes these variables produce. The results shown in Figures 2-5 are obtained with the geometry and mesh shown in Figure 1.

Figure 2 shows plots of the fill time and the fill time sensitivity versus inlet pressure. These results demonstrate that the fill time decreases with increasing inlet pressure, which follows the trend observed in the analytical solution for isothermal considerations as given by

$$t = \frac{\mu}{k}\frac{\Phi}{P_0}\left[\frac{R^2}{2}\ln\left(\frac{R}{R_0}\right) - \frac{R^2}{4} + \frac{R_0^2}{4}\right] \tag{60}$$

where, μ is viscosity; Φ, porosity; k, permeability; P_0, inlet pressure; R_0, inner radius; R, outer radius; t, time to fill from R_0 to R Figure 3 shows the fill time and the fill time sensitivity versus inlet flow rate. The results are as expected since the volume of the mold remains constant; and, the fill time decreases as inlet flow rate increases. Figure 4 is a plot of pressure at the mold inlet with respect to the inlet flow rate and it shows that inlet pressure is approximately a linear function of the inlet flow rate for the given range of values. One may expect pressure to be a linear function of injector flow rate as seen in Henz *et al.* (2003), but because of the combined temperature/cure effects on viscosity there is a small deviation from a constant sensitivity value in Figure 4. Figure 5 shows results unattainable from isothermal analysis. From the numerical results it is possible to plot the fill time and the fill time sensitivity versus inlet temperature. As expected, the fill time decreases as the inlet temperature increases because viscosity is a function of temperature, and the viscosity decreases with increasing temperature. Hence, from the isothermal analytical solutions one observes that as the viscosity decreases for a constant inlet pressure, so does the mold fill time. All of these results follow what is expected from experience and from representative isothermal analytical solutions. The sensitivity results also follow the expected trends for the specified boundary conditions. Although fill time may appear to be a linear function of inlet temperature in Figure 5 it is in fact nonlinear because of the constant pressure injection condition. The fill time with constant injection pressure is linearly

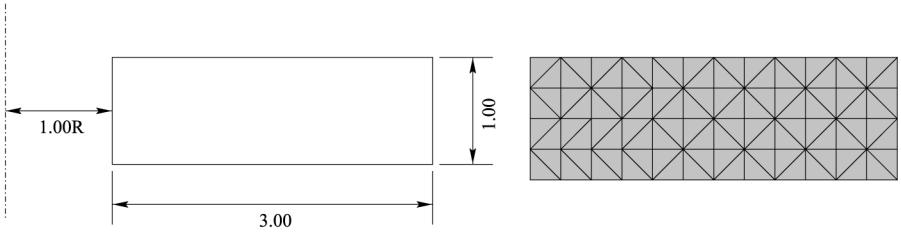

(a) 4.00"R disk with 1.00"R hole for non-isothermal RTM study

(b) Mesh of 4.00" disk with 1.00"R hole

Figure 1.
Example geometry and finite element mesh

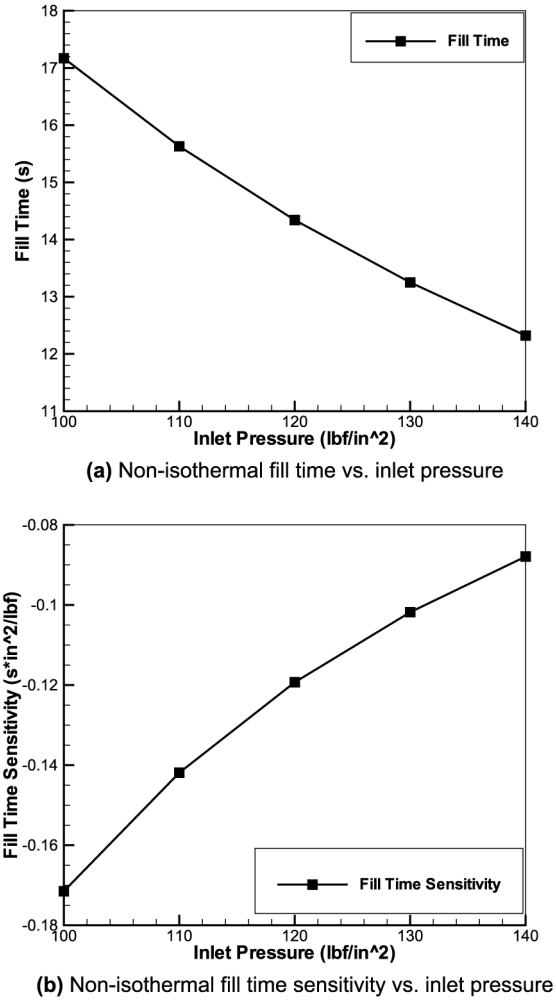

(a) Non-isothermal fill time vs. inlet pressure

(b) Non-isothermal fill time sensitivity vs. inlet pressure

Figure 2.
Non-isothermal fill time and fill time sensitivity vs inlet pressure plots for the 4.00 in. R disk model

dependent on resin viscosity, but viscosity in non-isothermal modeling is dependent on temperature and cure, which axe both affected by inlet temperature.

3.6 Verification of non-isothermal RTM sensitivity equations

Since there does not exist an available analytical solution for the non-isothermal filling process, the following definition of the derivative is employed:

$$\lim_{\Delta p \to 0} \frac{t_{\text{fill}}(p + \Delta p) - t_{\text{fill}}(p)}{\Delta p} = \frac{\partial t_{\text{fill}}}{\partial p} = \mathbf{S}_{t_{\text{fill}}} \tag{61}$$

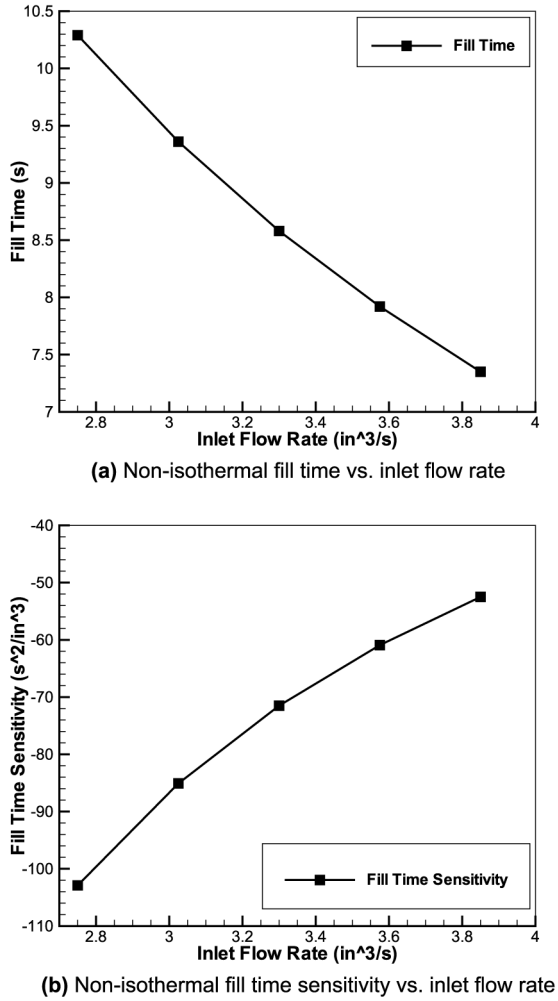

Figure 3.
Non-isothermal fill time and fill time sensitivity vs inlet flow rate plots for the 4.00 in. *R* disk model

The associated error calculation is taken as

$$\text{Error} = \frac{\Delta p \cdot \mathbf{S}_{t_{\text{fill}}}}{t_{\text{fill}}(p + \Delta p) - t_{\text{fill}}(p)} - 1.0 \tag{62}$$

where p and Δp are the value of the sensitivity parameter and the change in the sensitivity parameter, respectively (e.g. T_{inlet}). For verification purposes the error, as defined in equation (62), should monotonically approach zero as Δp decreases. Also, the results obtained from a Taylor series expansion, equation (63), should closely follow the numerical results for small changes in the sensitivity parameter, or graphically these results should be tangent to the solution of the numerical analysis obtained by employing repeated numerical simulations.

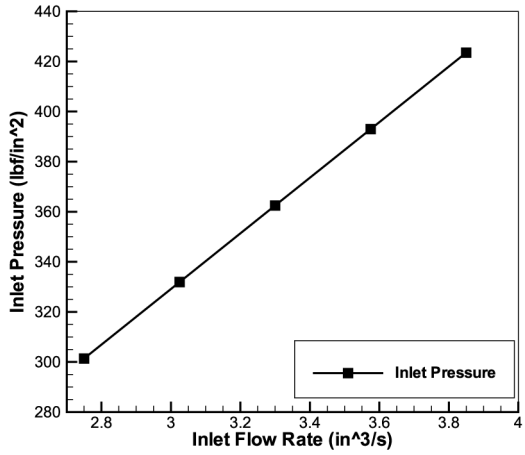

(a) Non-isothermal inlet pressure vs. inlet flow rate

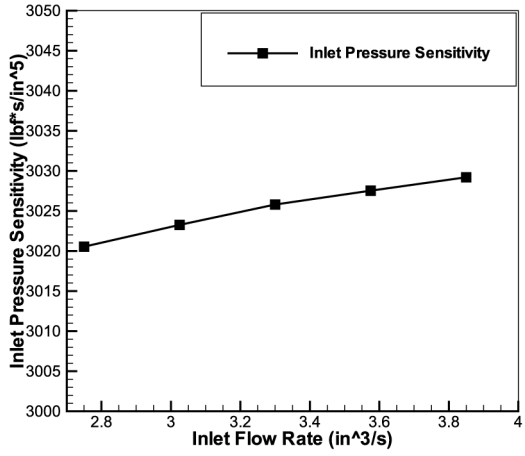

(b) Non-isothermal inlet pressure sensitivity vs. inlet flow rate

Figure 4.
Non-isothermal inlet pressure and inlet pressure sensitivity vs inlet flow rate plots for the 4.00 in. R disk model

The first-order Taylor series expansion is given as

$$w(p) = w(p_0) + \frac{\partial w}{\partial p}|_{p_0}(p - p_0) + \cdots \tag{63}$$

where w (p) is the numerical result and p is the sensitivity parameter. It is possible to include higher order terms in the Taylor series expansion to increase accuracy but the increase in computational complexity is typically not essential (Blackwell *et al.*, 1999a, b). The main impetus for computing the CSE is to find trends and to compare the effects of various parameters on the physical process in question. Note that the non-isothermal model verification in this section refers to the axi-symmetric model shown in Figure 6, with the following parameters

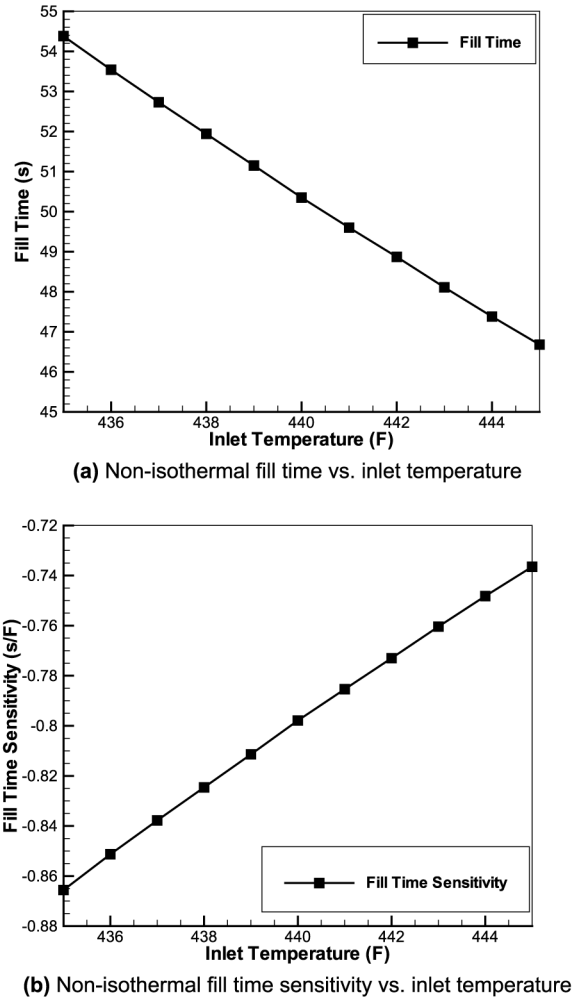

Figure 5.
Non-isothermal fill time and fill time sensitivity vs inlet temperature plots for the 4.00 in. R disk model

$$T_{\text{mold}} = 450.00°\text{F} \quad \Delta t = 0.01\,\text{s} \quad k = 5.300 \times 10^{-6}\,\text{in.}^2 \quad P_0 = 300.00\,\text{psi}$$

Figure 6 is used as a proof of concept for sensitivity analysis with complex geometries. Significant differences between the results observed here with the axi-symmetric model and future analysis of other complex geometries is not anticipated.

Since the focus of this work is non-isothermal RTM process modeling sensitivity, the verification is only performed here for the thermal sensitivity parameter of inlet temperature. For the verification of the inlet temperature sensitivity parameter, the Taylor series is used to compare the sensitivity results to the derivative of the fill time with respect to the inlet temperature. The original Taylor series assumed for estimating the fill time results is given as

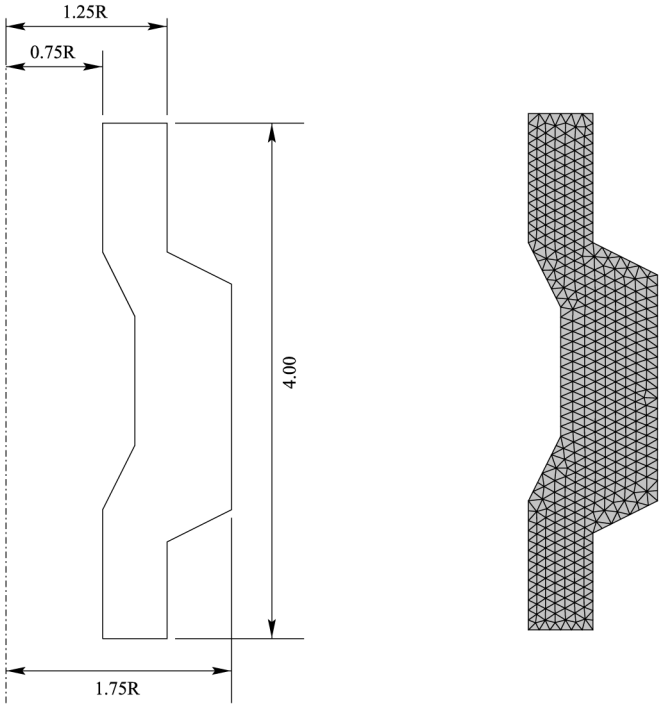

(a) Axi-symmetric part for verification study of non-isothemal RTM

(b) Axi symmetric part mesh for verification study of non-isothermal RTM

Figure 6.
Geometry and finite element mesh used for analytical/numerical comparison

$$t_{\text{fill}_1} = t_{\text{fill}_0} + \frac{\partial t_{\text{fill}}}{\partial T_{\text{inlet}}} \cdot \Delta T_{\text{inlet}} \tag{64}$$

In the first-order Taylor series estimation from equation (64), the resin viscosity is not explicitly included. The viscosity term is instead encapsulated inside the fill time sensitivity term, $\partial t_{\text{fill}}/\partial T_{\text{inlet}}$ in equation (64). Viscosity is a function of the temperature profile inside of the part, which in turn is a function of the inlet temperature. This dependence of the temperature profile on the inlet temperature gives the viscosity term a reliance on inlet temperature which is used to define a new Taylor series dependent on viscosity. In order to explicitly list the viscosity in the Taylor series expansion the following modified Taylor series is used, which is based on the viscosity sensitivity.

$$t_{\text{fill}_1} = t_{\text{fill}_0} + \frac{\partial t_{\text{fill}}}{\partial \mu} \cdot \Delta \mu \tag{65}$$

The $\Delta\mu$ term is computed for every filled node in the numerical model at each filling time step. The final $\Delta\mu$ used in the Taylor series is a weighted average of each time step, weighted by the volume filled at the respective time step. The reason for using the fill time sensitivity with respect to viscosity is that the fill time is a direct function of viscosity rather than that of inlet temperature. This fact is reflected in the calculations

performed and equation (66), where viscosity is the only filling parameter calculated with the results from the thermal analysis.

$$t_{\text{fill}_1} = t_{\text{fill}_0} + \frac{\partial t_{\text{fill}}}{\partial \mu}\frac{\partial \mu}{\partial T}\frac{\partial T}{\partial T_{\text{inlet}}} \cdot \Delta T_{\text{inlet}} \tag{66}$$

The new method described by equation (65) for estimating the fill times shows reduced error with the modification presented when compared to the method from equation (64), for multiple temperature ranges. The results using equations (64) and (65) are shown graphically in Figures 7-9 for inlet temperatures of 300, 350, and 420°, respectively. In the legends, T_{inlet} refers to the Taylor series initially used for the error estimation, and viscosity and T_{inlet} refers to the modified Taylor series estimation. The lines representing the viscosity based estimations more closely follow the finite element results than the lines that represent the Taylor series estimation with inlet

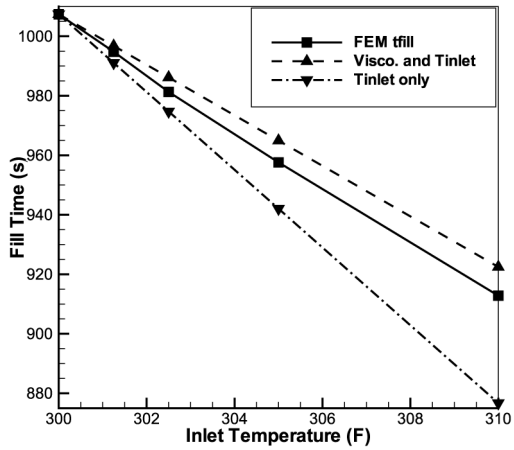

Figure 7.
Comparison of the two methods for estimating fill time for $T_{\text{inlet}} = 300.0$°F, for the axi-symmetric verification model

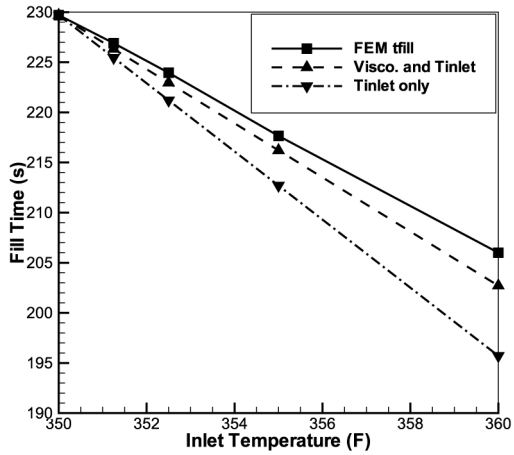

Figure 8.
Comparison of the two methods for estimating fill time for $T_{\text{inlet}} = 350.0$°F, for the axi-symmetric verification model

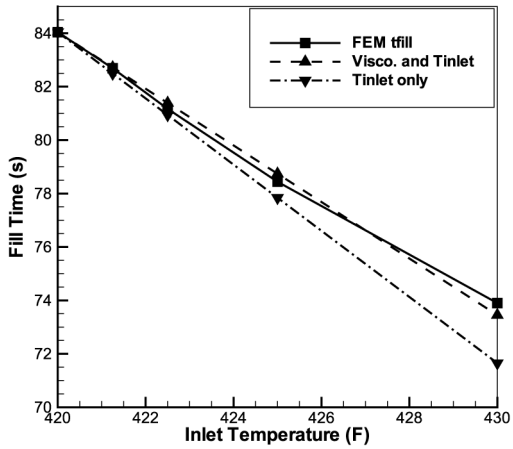

Figure 9.
Comparison of the two methods for estimating fill time for $T_{inlet} = 420.0°F$, for the axi-symmetric verification model

temperature only. It is observed that the viscosity and inlet temperature line do not always fall below the finite element results, i.e. tangent to the results curve. For constant injection pressure boundary conditions the mold fill time is dependent upon the resin viscosity within the mold. The resin viscosity is in turn a function of temperature and degree of resin cure, and therefore a function of inlet temperature. This indirect effect of inlet temperature on mold fill time translates into the fact that there will be some error accumulated in the results presented.

In this work, the authors have investigated the sensitivity of RTM processing parameters such as fill time and mold temperature with respect to constant variables including inlet pressure, flow rate, permeability, etc. There are cases when these variables are not constants but rather complex functions dependent upon other variables and may be non-linear. In cases such as this, the CSE can be still utilized but requires the use of an iterative solution method for the resulting CSE. In these instances other methods such as the automatic differentiation scheme as discussed in Borggaard and Verna (2000) may be utilized efficiently but are by no means required or even advisable if the CSE is already available for the current problem.

4. Concluding remarks

In this paper, the CSE has been developed for the first time for non-isothermal considerations in RTM process modeling. This includes the non-isothermal RTM filling CSE, the temperature CSE, and the cure CSE. Sensitivity parameters have been examined for the cases of material properties, boundary conditions, and geometric parameters. Numerical results were presented for an example axi-symmetric model and discussed. Finally, the fill time sensitivity results for the non-isothermal RTM numerical model were validated. This was accomplished by modifying the Taylor series initially used to estimate the fill time for small changes in inlet temperature as given in equation (64), with the modified Taylor series given in equation (65). The results using the modified Taylor series indicate that the dependence of fill time on inlet temperature is not direct but rather is a side effect of changes in viscosity.

References

Blackwell, B.F., Dowding, K.J. and Cochran, R.J. (1999a), "Development and implementation of sensitivity coefficient equations for heat conduction problems", *Numerical Heat Transfer, Part B*, Vol. 36, pp. 15-32.

Blackwell, B.F., Dowding, K.J. and Cochran, R.J. (1999b), "Application of sensitivity coefficients for heat conduction problems", *Numerical Heat Transfer, Part B*, Vol. 36, pp. 33-55.

Borggaard, J. and Verna, A. (2000), "On efficient solutions to the continuous sensitivity equation using automatic differentiation", *SIAM Journal on Scientific Computing*, Vol. 22 No. 1, pp. 39-62.

Brooks, A.N. and Hughes, T.J.R. (1982), "Streamline upwind/Petrov-Galerkin formulations for convection dominated flows with particular emphasis on the incompressible Navier-stokes equations", *Computer Methods in Applied Mechanics and Engineering*, Vol. 32, pp. 199-259.

Castro, J.M. and Macosko, C.W. (1980), "Kinetics and rheology of typical polyurethane reaction injection molding systems", paper presented at Society of Plastics Engineering Annual Technical Conference, Vol. 26, pp. 434-8.

Dusi, M.R., Lee, W.I., Ciriscioli, P.R. and Springer, G.S. (1987), "Cure kinetics and viscosity of Fiberite 976 resin", *Journal of Composite Materials*, Vol. 21 No. 3, pp. 243-61.

Henz, B.J., Tamma, K.K., Kanapady, R., Ngo, N.D. and Chung, P.W. (2003), "Process modeling of composites by resin transfer molding: practical applications of sensitivity analysis for isothermal considerations", *International Journal of Numerical Methods for Heat & Fluid Flow*, Vol. 13 No. 4, pp. 415-47.

Kamal, M.R. and Sourour, S. (1973a), "Integrated thermo-rheological analysis of the cure of thermosets", *SPE Technical Paper*, Vol. 18 No. 187.

Kamal, M.R. and Sourour, S. (1973b), "Kinetics and thermal characterization of thermoset cure", *Polymer Engineering and Science*, Vol. 13, pp. 59-64.

Kamal, M.R. and Sourourm, S. (1973c), *SPE Technical Paper*, Vol. 13 No. 59.

Kaviany, M. (1991), *Principles of Heat Transfer on Porous Media*, Springer-Verlag, New York, NY.

Lee, L.J., Young, W.B. and Lin, R.J. (1994), "Mold filling and cure modeling of RTM and SRIM processes", *Composite Structures*, Vol. 27, pp. 109-20.

Lim, S.T. and Lee, W.I. (2000), "An analysis of the three-dimensional resin-transfer mold filling process", *Composites Science and Technology*, Vol. 60, pp. 961-75.

Mathur, R., Advani, S.G. and Fink, B.K. (2000), "A sensitivity-based gate location algorithm for optimal mold filling during the resin transfer molding process", Tech. Rep., US Army Research Laboratory, Aberdeen Proving Grounds, Aberdeen, MD.

Mohan, R.V., Ngo, N.D. and Tamma, K.K. (1999), "On a pure finite-element-based methodology for resin transfer mold filling simulations", *Polymer Engineering and Science*, Vol. 39 No. 1.

Ngo, N.D. and Tamma, K.K. (2004), "An integrated comprehensive approach to the modeling of resin transfer molded composite manufactured net-shaped parts", *Computer Modeling in Engineering & Sciences*, Vol. 5 No. 2, pp. 103-133.

Ngo, N.D., Mohan, R.V., Chung, P.W. and Tamma, K.K. (1998), "Recent developments encompassing non-isothermal/isothermal liquid composite molding process modeling/analysis: physically accurate, computationally effective and affordable simulations and validations", *Journal of Thermoplastic Composite Materials*, Vol. 11 No. 6, pp. 493-532.

Shojaei, A., Ghaffarian, S.R. and Karimian, S.M.H. (2003), "Simulation of the three-dimensional non-isothermal mold filling process in resin transfer molding", *Composites Science and Technology*, Vol. 63, pp. 1931-48.

Sourour, S. and Kamal, M.R. (1972), *SPE Technical Paper*, Vol. 18 No. 93.

Further reading

Henz, B.J., Kanapady, R., Ngo, N., Chung, P. and Tamma, K.K. (2000), "Simulation based design and visualization tools: sensitivity coefficients for advanced composites manufacturing", *AHPCRC Bulletin*, Vol. 10, pp. 18-20.

Huebner, K.H., Thorton, E.A. and Byrom, T.G. (1995), *The Finite Element for Engineers*, Wiley, New York, NY.

Pelletier, D., Borggaard, J. and Hetú, J-F. (2000), "A continuous sensitivity equation method for conduction and phase change problems", paper presented at 38th AIAA Aerospace Sciences Meeting and Exhibit, American Institute of Aeronautics and Astronautics, Reston, VA, Reno, NV, 10-13 January.

Stanley, L.G. (2000), "A sensitivity equation method for modeling processes", paper presented at IEEE International Conference on Control Applications, Institute of Electrical and Electronics Engineers, Inc., Piscataway, NJ, Anchorage, AK, 25-27 September.